Supporting Information for

Liquid-Phase Syntheses and Material Properties of Two Dimensional Nanocrystals of Rare Earth-Selenium Compound Containing Planar Se-Layers: $RESe_2$ Nanosheets and $RE_4O_4Se_3$ Nanoplates

Jun Gu,[‡] Ze-Qiong Zhao,[‡] Yi Ding,[†] Hong-Liang Chen, Ya-Wen Zhang* and Chun-Hua Yan*

Beijing National Laboratory for Molecular Science, State Key Laboratory of Rare Earth Materials and Applications, PKU-HKU Joint Laboratory in Rare Earth Materials and Bioinorganic Chemistry, College of Chemistry and Molecular Engineering, Peking University, Beijing 100871, China.

[†]Present address: Department of Materials Science and Engineering, Massachusetts Institute of Technology, Cambridge, Massachusetts 02139, USA.

Supplementary Data

Table S1. Reaction conditions for the syntheses of $RESe_2$ and $RE_4O_4Se_3$ NCs.

	SeO_2 (g)	Temperature (℃)	Duration (min)
$LaSe_2$ nanosheets	0.222	310	1~30[a]
$CeSe_2$ nanosheets	0.222	320	30[b]
$PrSe_2$ nanosheets	0.222	310	60[b]
$NdSe_2$ nanosheets	0.444	320	60[b]
$EuSe_2$ nanobars	0.222	310	60[b]
$Nd_4O_4Se_3$ nanoplates	0.444	310	60[b]
$Sm_4O_4Se_3$ nanoplates	0.444	310	60[b]
$Gd_4O_4Se_3$ nanoplates	0.444	310	60[b]
$Tb_4O_4Se_3$ nanoplates	0.444	310	60[b]
$Dy_4O_4Se_3$ nanoplates	0.444	310	60[b]
$Ho_4O_4Se_3$ nanoplates	0.444	310	60[b]

[a]The duration of heating after the reaction mixture turned black. [b] The duration of heating after the temperatures reached the target temperatures.

Table S2. EDS analysis results of $RESe_2$ NCs (RE = Ce, Pr, Nd, Eu).

	$CeSe_2$	$PrSe_2$	$NdSe_2$	$EuSe_2$
Mole ratio of RE:Se	32:68	41:59	39:61	35:65

Table S3. XRD peaks of orthorhombic $Nd_4O_4Se_3$ calculated from ref 29.

2θ (degree)	***d* (Å)**	**Intensity (a. u.)**	***h k l***
25.21	3.530	78.5	2 0 2
30.63	2.916	100	0 1 3
31.59	2.830	75.0	2 1 1
34.74	2.581	10.6	3 0 2
35.09	2.555	41.3	2 0 4
37.43	2.401	5.0	2 1 3
39.75	2.266	14.1	3 1 1
42.24	2.138	19.0	0 0 6
42.74	2.114	10.3	4 0 0
45.12	2.008	7.8	4 0 2
45.45	1.994	25.5	0 2 0
47.26	1.922	24.9	2 1 5
49.26	1.848	12.9	4 1 1
51.75	1.765	5.8	4 0 4
52.68	1.736	11.6	2 2 2
53.49	1.712	17.5	4 1 3
58.69	1.572	11.8	2 2 4
59.63	1.549	13.8	2 1 7
61.35	1.510	5.1	4 1 5
63.78	1.458	6.7	0 2 6
64.15	1.451	6.0	4 2 0
71.26	1.322	8.4	0 3 1
72.16	1.308	5.3	4 1 7
74.72	1.269	6.7	0 3 3

Table S4. Elemental analysis results (mass fraction) of $Nd_4O_4Se_3$ nanoplates and $Gd_4O_4Se_3$ nanoplates.

	C	H	N	O (from OA)
$Nd_4O_4Se_3$	22.0%	3.5%	0.1%	2.9%
$Gd_4O_4Se_3$	48.2%	7.6%	1.2%	4.5%

Table S5. Atomic ratios of C:O:Se of $Nd_4O_4Se_3$ nanoplates and $Gd_4O_4Se_3$ nanoplates obtained from XPS analysis.

	C	O	Se
$Nd_4O_4Se_3$	81.6%	13.3%	5.1%
$Gd_4O_4Se_3$	89.5%	8.5%	1.9%

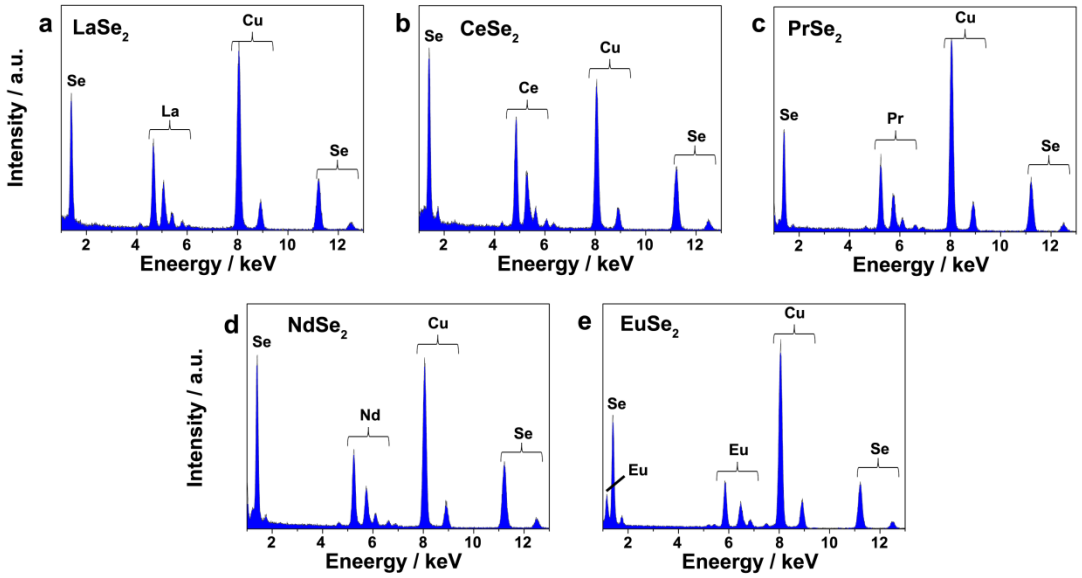

Figure S1. EDS analyses of $RESe_2$ (RE = La to Nd, Eu) NCs.

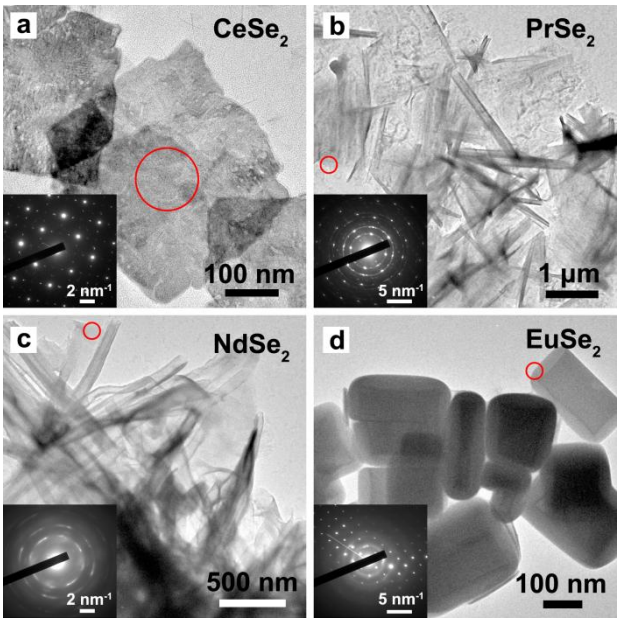

Figure S2.TEM images and SAED patterns of $RESe_2$ (RE = Ce, Pr, Nd, Eu) NCs. Red circles indicate the selected area for electron diffraction.

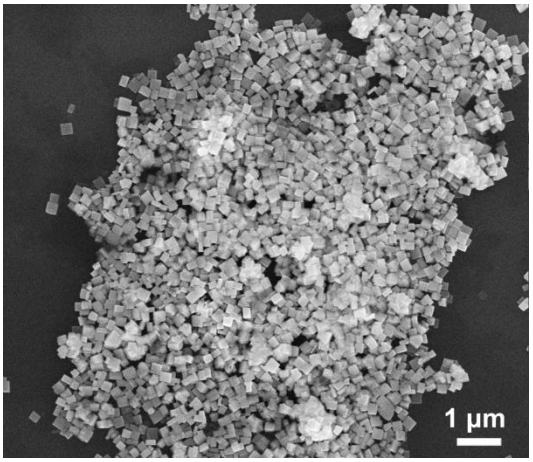

Figure S3. SEM micrograph of $EuSe_2$ nanobars.

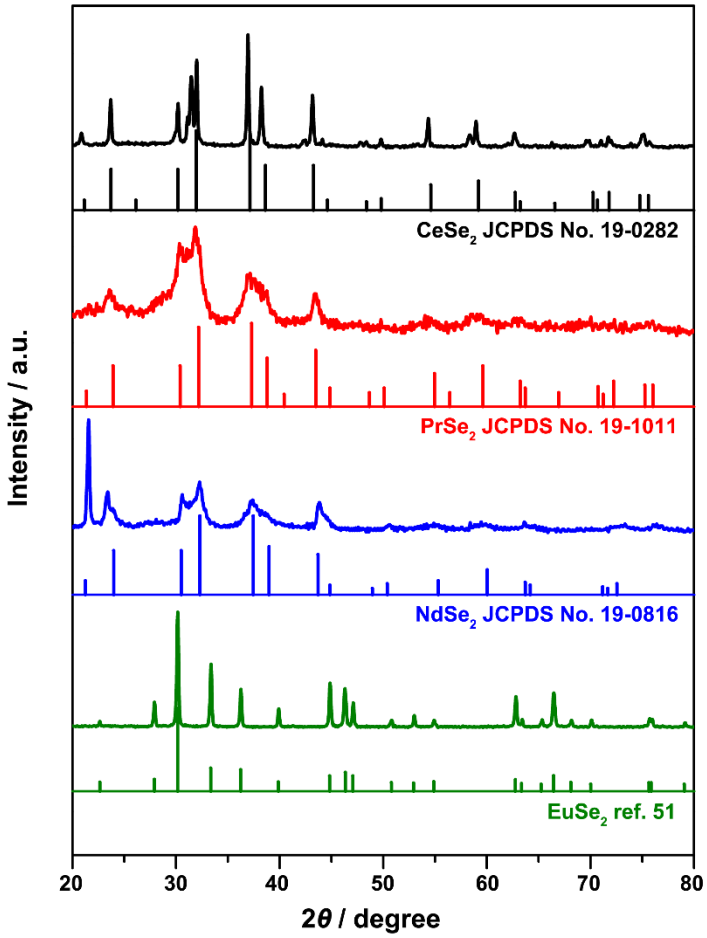

Figure S4. XRD patterns of $RESe_2$ NCs compared with standard XRD patterns (orthorhombic $CeSe_2$, JCPDS No. 19-0282; orthorhombic $PrSe_2$, JCPDS No. 19-1011; orthorhombic $NdSe_2$, JCPDS No. 19-0816; tetragonal $EuSe_2$, data from ref. 51).

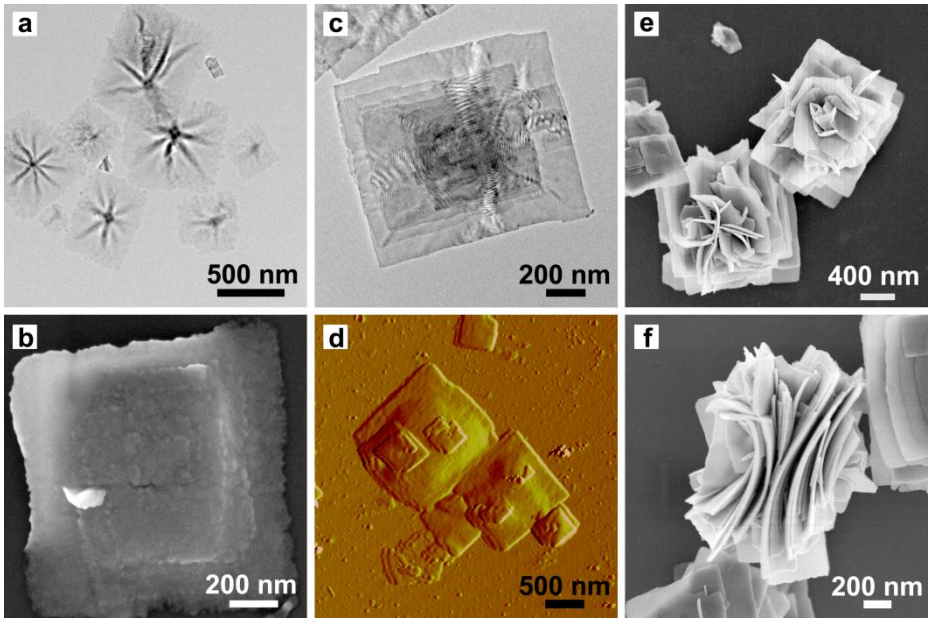

Figure S5. Morphology characterization of $LaSe_2$ nanosheets obtained with different growth durations: 1 min: (a) TEM image and (b) SEM micrograph; 15 min: (c) TEM image and (d) AFM phase image; 30 min: (e and f) SEM micrographs.

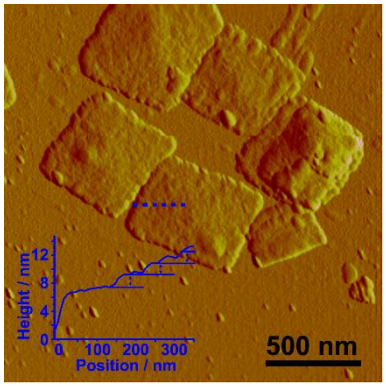

Figure S6. AFM phase image of $LaSe_2$ nanosheets (growth duration: 1 min) after thermal treatment in air at 300 ℃ for 30 min. Inset shows the height diagram along the blue dashed line.

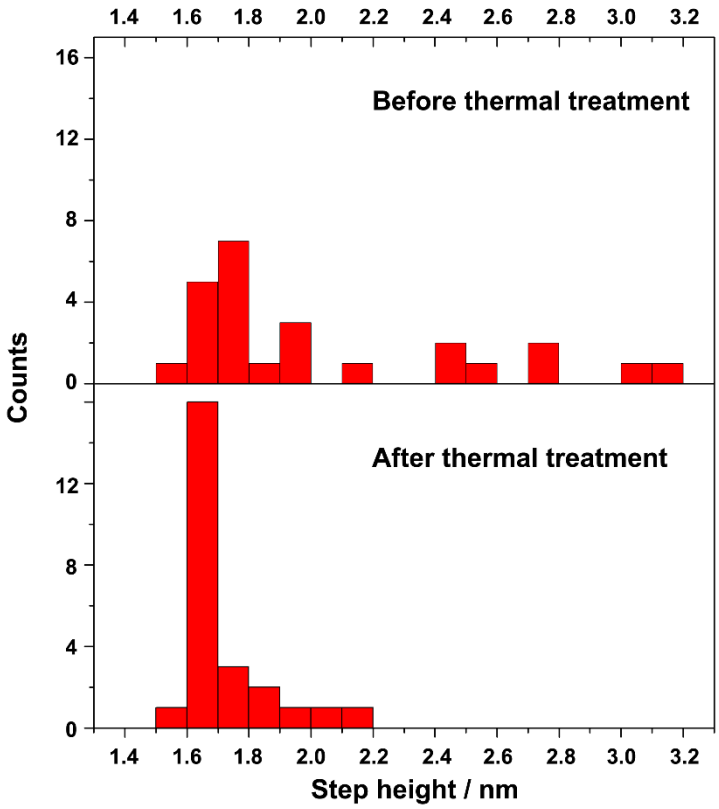

Figure S7. Statistical results of the height of the steps on $LaSe_2$ nanosheets before and after thermal treatment collected from AFM measurements.

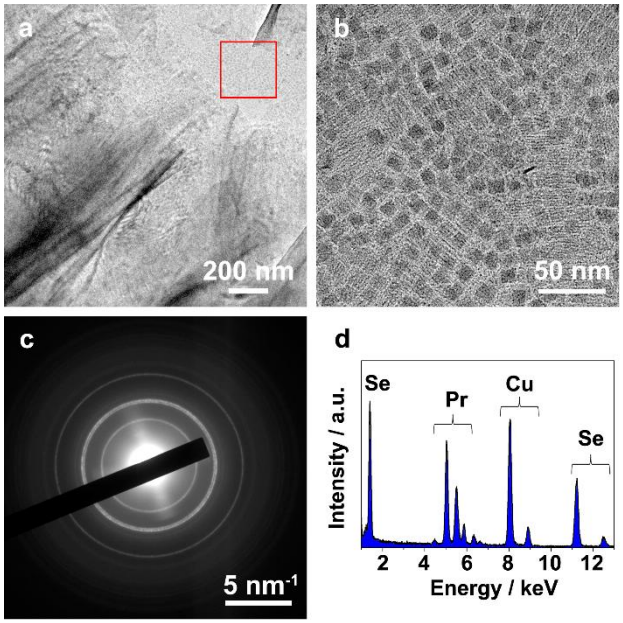

Figure S8. (a) TEM image of the mixture of $PrSe_2$ nanosheets and $Pr_4O_4Se_3$ nanoplates; (b) Higher-magnification TEM image of the area enclosed by red square in (a); (c) SAED pattern of the area in (b); (d) EDS analysis of the mixed sample.

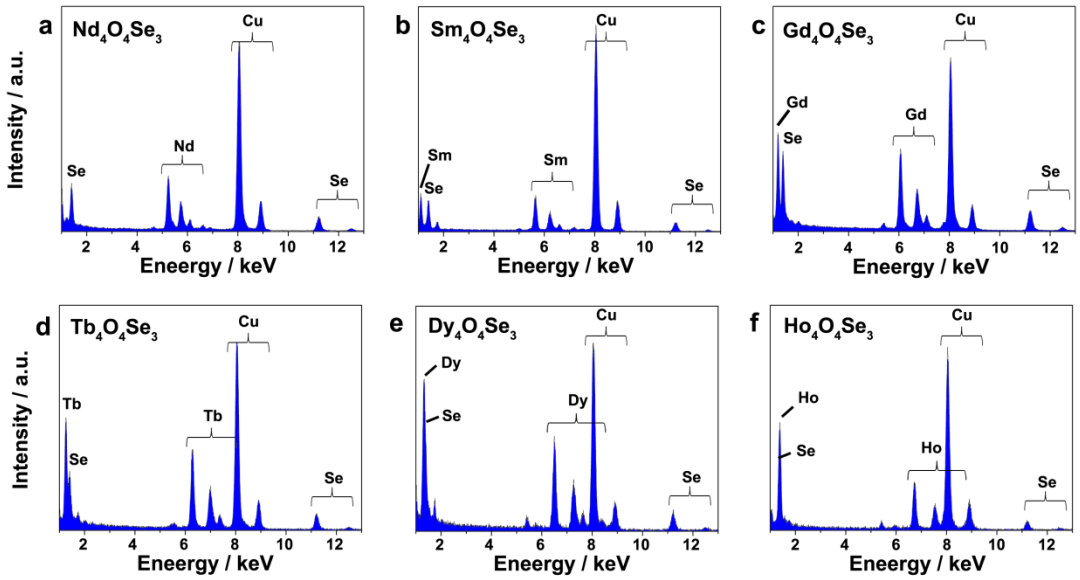

Figure S9. EDS analyses of $RE_4O_4Se_3$ (RE = Nd, Sm, Gd to Ho) nanoplates.

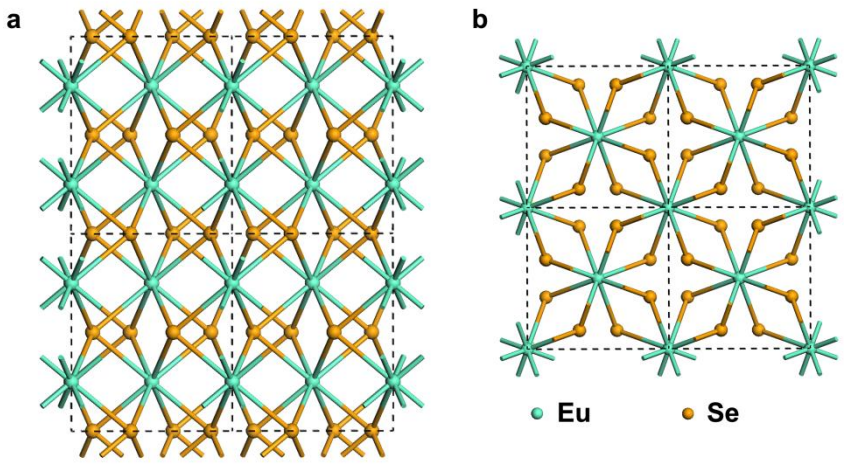

Figure S10. Crystal structure of tetragonal $EuSe_2$: (a) side view and (b) top view.

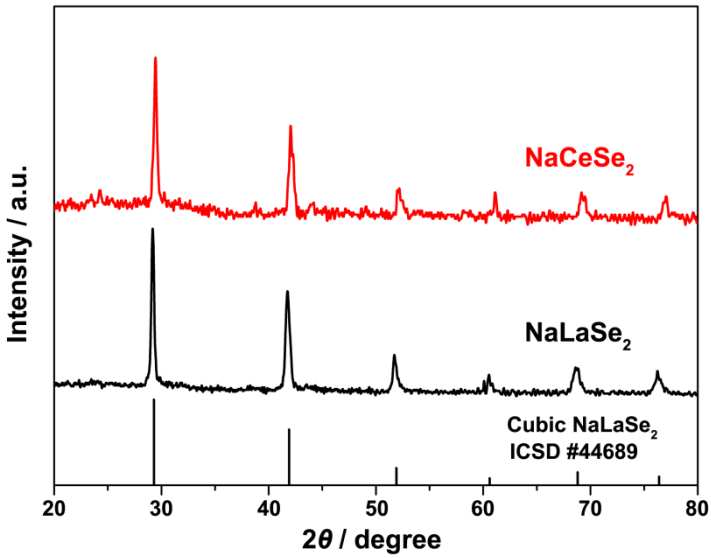

Figure S11. XRD patterns of $NaLaSe_2$ and $NaCeSe_2$ NCs, compared with the standard XRD pattern of cubic $NaLaSe_2$ (calculated from the crystallographic data of ICSD #44689).

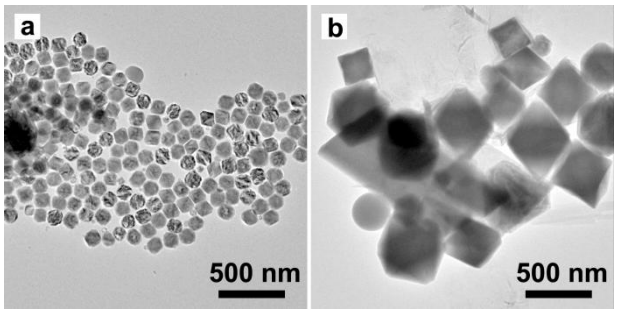

Figure S12. TEM images of $NaLaSe_2$ and $NaCeSe_2$ NCs.

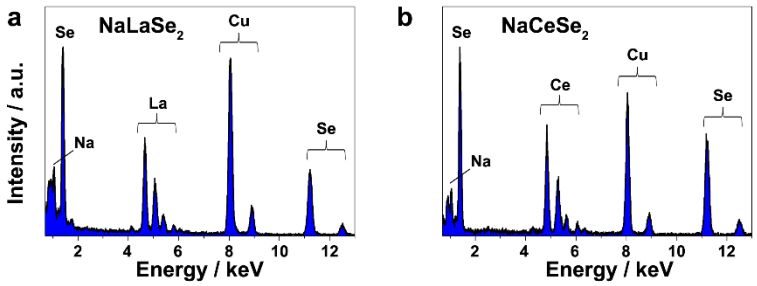

Figure S13. EDS analyses of $NaRESe_2$ (RE = La and Ce) NCs.

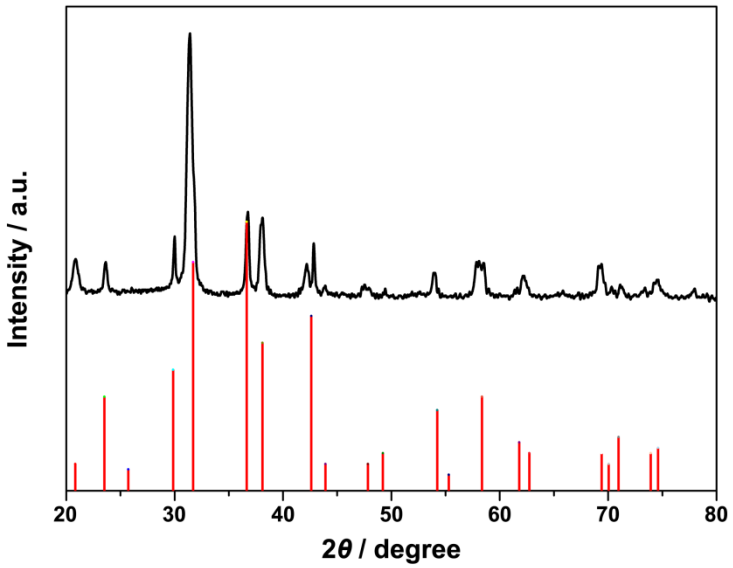

Figure S14. XRD pattern of $LaSe_2$ nanosheets after thermal treatment compared with the standard XRD pattern of $LaSe_2$.

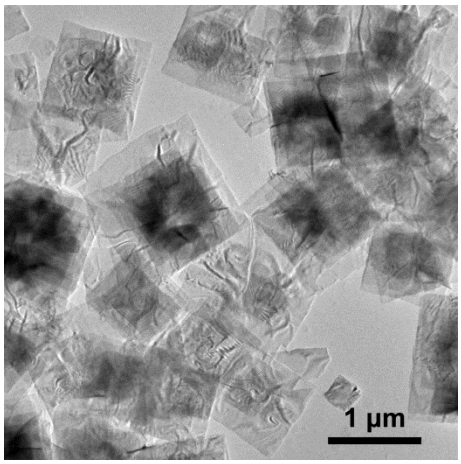

Figure S15. TEM image of $LaSe_2$ nanosheets after thermal treatment.

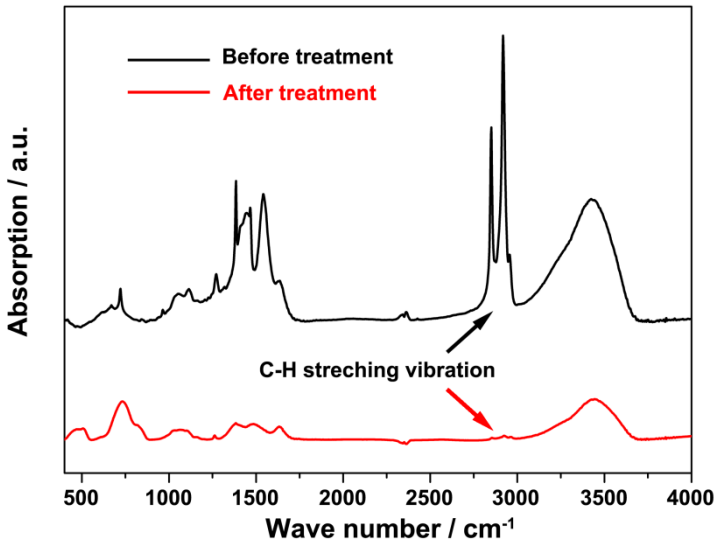

Figure S16. FTIR spectra of $LaSe_2$ nanosheets before and after thermal treatment.

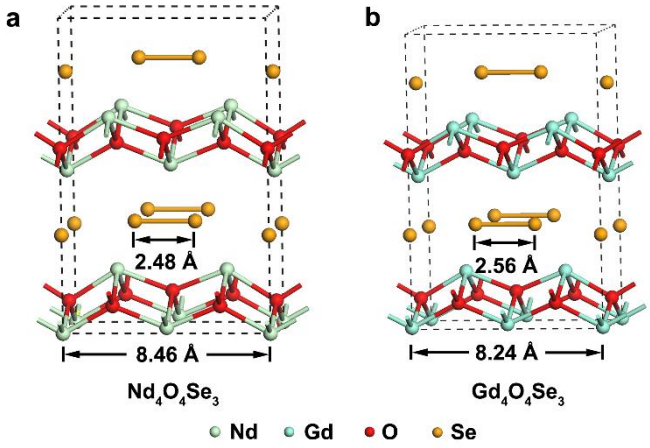

Figure S17. Structure optimization results of orthorhombic $Nd_4O_4Se_3$ (a) and $Gd_4O_4Se_3$ (b) using DFT simulation. The DFT simulation was performed on Vienna Ab-initio Simulation Package (VASP, version 5.2). General gradient approximation (GGA) was used in the exchange-correlation functional. Projected augmented wave (PAW) pseudopotential was introduced. The energy cut-off for the plane-wave basis was 500 eV. During the structure optimization, the lattice parameters were fixed and atomic coordinates were allowed to relax.